Food and Chemical Toxicology 133 (2019) 110753

Contents lists available at ScienceDirect

Food and Chemical Toxicology

journal homepage: www.elsevier.com/locate/foodchemtox

More data on *in vitro* assessment of comparative and combined toxicity of metal oxide nanoparticles

Tatiana Bushueva[a], Ilzira Minigalieva[a], Vladimir Panov[b], Alisa Kuznetsova[a], Anna Naumova[a], Vladimir Shur[c], Ekaterina Shishkina[c], Vladimir Gurvich[a], Larisa Privalova[a], Boris Katsnelson[a,*]

[a] Medical Research Center for Prophylaxis and Health Protection in Industrial Workers, Ekaterinburg, 620014, Russia
[b] Institute of Industrial Ecology, The Urals Branch of the Russian Academy of Sciences, Ekaterinburg, Russia
[c] School of Natural Sciences and Mathematics, The Ural Federal University, Ekaterinburg, Russia

ARTICLE INFO

Keywords:
Lead oxide
Copper oxide
Nanoparticles
in vitro toxicity

ABSTRACT

Isolated and combined damaging effects of PbO and CuO nanoparticles were estimated on an established line of human fibroblasts by a decrease in: (a) the cellular dehydrogenase activity (MTT Assay), (b) the ATP content (Luminescent Cell Viability Assay), (c) the cellular proliferation, viability, spreading, and attachment to substrate evaluated integrally by continuous impedance-based measurement of the Normalized Cell Index. Using all these indices, we demonstrate an explicit dependence of cell damage on the concentrations of both metal oxide nanoparticle (MeO-NP) species. This dependence is adequately approximated with a hyperbolic function. At equal exposure levels, PbO-NP and CuO-NP demonstrate quantitatively similar cytotoxicities. The same was observed previously for some non-specific *in vivo* toxicity measures. The combined *in vitro* cytotoxicity has also been described mathematically using the Response Surface Methodology and found to be represented by various types, thus corroborating, in this respect also, the findings of a previous animal experiment with the same MeO-NPs.

1. Introduction

Nanoparticles (NP) of metals (Me-NP) and especially of their oxides (MeO-NP) are of special interest in the light of health risk assessment and management because, along with so-called engineered NPs having many important technical, agronomical and medical uses Piperigkou et al. (2016); Fernández-Bertólez et al. (2018); Henrich-Noack P. et al., 2019, there can be usually detected a substantial fraction of nanoscale ("ultrafine") particles in the condensation aerosols generated by many traditional technologies Katsnelson et al. (2017); Minigalieva et al. (2017b); Kirichenko et al., (2018). It should be kept in mind, however, that such technologies as steel making (alloyed steels especially), electric arc welding, pyrometallurgy of heavy nonferrous metals (particularly copper smelting and refining) pollute workroom and ambient air with multicomponent (polymetallic) particulates and, thus, create multiple occupational risks for human health due to exposure to toxic MeO-MP Katsnelson et al. (2017); Minigalieva et al. (2017b).

Meantime, while most of the published research in the field of nanotoxicology has been performed *in vitro* (mainly on cultures of stable cell lines), our team acting in collaboration with investigators from the Center for Medical Research of the Medical University of Graz (Austria) seems to be the first to be using such experimental modeling for estimating the *comparative and combined toxicity* of nanoparticles. Moreover, we are not aware of anyone else to have raised the question of whether respective estimates obtained *in vitro* for some nanoparticles agree in principle with those based on animal experiments involving the same nanoparticles Minigalieva et al. (2017a).

For that study, we chose Mn_3O_4-NP and NiO-NP, a typical combination for some welding fumes, and demonstrated that damage to different human cell lines quantitatively depended on MeO-NP concentrations. Mn_3O_4-NP was found to be more cytotoxic than NiO-NP, thus corroborating the comparative *unspecific* toxicity estimates obtained for these MeO-NPs in our animal experiments. The same is true of combined toxicity patterns in the sense that their variability is determined by many factors e.g. Minigalieva et al. (2017b), an inherent feature found in the combined cytotoxicity of the MeO-NPs studied both *in vitro* and *in vivo*. However, no correspondence has been found between the effects of a particular type of combined action on a whole organism and on a cell culture. Thus, for example, considering the fact of manganese-specific *in vivo* brain damage (including different stages of basal nuclei cells degeneration) proved previously, *in vitro* experiments on neurons revealed just a slight enhancing effect of Mn_3O_4-NP

* Corresponding author. DSci - 30 Popov Str, Ekaterinburg, 620014, Russia.
E-mail addresses: bkaznelson@etel.ru, bkaznelson@ymrc.ru (B. Katsnelson).

https://doi.org/10.1016/j.fct.2019.110753
Received 4 April 2019; Received in revised form 5 August 2019; Accepted 6 August 2019
Available online 07 August 2019

on the action of NiO-NP, the dominant component in the combination Minigalieva et al. (2017a). This finding, however, was contrary to *in vivo* experimental data. In toto, we concluded that (a) *in vitro* tests could have a prognostic value, but only where the comparative non-specific toxicity of various MeO-NPs *in vivo* is at issue, and (b) for relevant characterization of MeO-NPs combined toxic action in occupational health terms, experiments on laboratory animals seem to be a more informative tool than experiments on cell cultures. A lack of correspondence between *in vitro* and *in vivo* assessments of gold nanoparticles genotoxicity was also demonstrated by Ávalos et al. (2018). On the other hand, Ghosh et al. (2016) found a good co-relation between the two biological systems as concerns toxicity characterization of ZnO nanoparticles.

We do realize, however, that the above statements might appear too categorical given a restricted actual experience they are derived from, and that the problem under consideration is important enough to be delved deeper. It should be stressed that experimental modeling of real-life exposure scenarios Tsatsakis et al. (2016), 2018 demands multi-factorial designs rather than isolated ones.

For our new study, we have chosen the pair CuO-NP and PbO-NP, which is characteristic of condensation aerosols polluting air in and around copper smelters and copper fire refineries Katsnelson et al. (2017) and is therefore of considerable practical interest.

In the recent literature, extensive data is available for toxicological characterization of CuO–NP, obtained on different experimental models Karlsson et al. (2008); Studer et al. (2010); Bondarenko et al. (2012); Pang et al. (2012); Magaye et al. (2012); Xu et al., 2013; Sizova et al. (2012); Gomes et al. (2013); Alarifi et al. (2013); Cronholm et al., 2013; Cuillel et al. (2014); Privalova et al. (2014); etc. Toxicological studies of PbO-NP began much later Amiri et al. (2016); Dumková et al. (2017); Minigalieva et al. (2017c); Miri et al. (2018); Ng et al. (2019). To summarize briefly, as well as causing many widely recognized non-specific *in vivo* toxic effects common to virtually all Me-NPs and MeO-NPs studied to date (such as hepato-, spleno- and tubular nephrotoxicity, poly-organic genotoxicity, free radical formation, etc.) and cytotoxicity effects common to any cell type *in vitro,* each of the MeO-NPs under consideration induces *in vivo* some important damaging effect which is qualitatively specific for the respective toxic metal regardless of its chemical form Katsnelson et al. (2017). Thus, subchronic intoxication of rats with PbO-NP was observed to cause typical disturbances of porphyrin synthesis leading to anemia Minigalieva et al., 2017c while CuO-NP evoked a syndrome similar to Wilson's disease Privalova et al. (2014). As for the action of CuO + PbO in combination, we know only our own subchronic animal experiment Minigalieva et al. (2017c). Some of its results will be used in the Discussion of the present work. We are not aware of any *in vitro* studies *of* CuO + PbO combined toxicity at all. So, this scarcity of relevant data motivated our present study.

Regrettably, we have not yet found an adequate *in vitro* counterpart for the above-mentioned specific *in vivo* effects of PbO-NP or CuO-NP. Nevertheless, we deemed it worthwhile to estimate, for the time being, their non-specific comparative and combined cytotoxicities on one of the target cell cultures most widely used in such experiments, namely, the human fibroblast (partly compensating for this restriction by the use of several measures of cell damage).

2. Materials and methods

2.1. Preparation and characterization of nanoparticles

For this experiment, we prepared suspensions of MeO-NPs by laser ablation of 99.9% pure metal targets under deionized water (for technical details, see Katsnelson et al, 2015). The concentration of the suspensions was increased to 0.5 mg/mL by partial evaporation of the primary suspensions for 5 h at 50 °C. A scanning electron microscope (SEM), Cross Beam Workstation Auriga (Carl Zeiss, Germany), was used for the visualization of the nanoparticles. The NPs in both suspensions were of spherical shape[1] (Figs. 1 and 2) and had the mean diameters 24.5 ± 4.8 nm for CuO-NP and 47.0 ± 16.0 nm for PbO-NP. Their chemical composition was determined by Raman Spectroscopy performed with the help of a Raman confocal microscope, Alpha 300 AR (Germany), and proved to be just CuO and PbO.

The absence of any noticeable changes in the zeta potential as well as in the shape and position of the plasmon resonance peak two weeks after suspension preparation confirmed the satisfactory stability of the suspensions.

2.2. Cell exposure parameters and cytotoxicity estimates

The experiments were performed on a FLECH-104 cell line of human lung-derived embryonic fibroblasts from the bank of cell cultures by BioloT Ltd., Saint Petersburg, Russia. It presents a monolayer culture of fibroblast-like cells obtained from the lungs of an eight-week human embryo. The cell culture was kept at 37°C under an atmosphere of 5% CO_2 in a DMEM medium with L-glutamine, 1 g/L glucose, 10% fetal bovine serum (FBS), and 0.5% gentamicin antibiotic. We found previously that adding FBS to the DMEM as well as to other widely used cultural media significantly modified both solubilization and cytotoxicity effects of Mn_3O_4-NP and NiO-NP Minigalieva et al., 2017a and connected this phenomenon with the probable formation of the proten bio-corona (see, for instance, a comprehensive review by Neagu et al., 2017). That is why wee, keeping in mind making the conditions of an *in vitro* assay a closer approximation to *in vivo* conditions,[2] decided to use in this new study the (DMEM plus FBS) medium only.

The cells were seeded on a 96-well plate (TPP Techno Plastic Products AG, Trasadingen, Switzerland) for testing the dehydrogenase activity or ATP content, and on an 8-well plate (ACEA Biosciences, San Diego, California, USA) for determining the cell index, 70 000 cells per well in 100 μL of the medium and were incubated under an atmosphere of 5% CO_2 at 37 °C for 24 h before adding MeO-NPs. Incubation with these particles was conducted under the same conditions for 24 h. The final concentrations of nanoparticles in the incubation medium with concurrently exposed samples was 50–75 – 100–200 – 250–300 μg/mL. All exposure variants were performed in quadruplicates.[3]

The cytotoxic effect of such incubation was estimated quantitatively by three indices: the ATP content of the culture as per the luminescent signal, dehydrogenase activity in the MTT-assay, and determination of the Normalized Cell Index.

The ATP bioluminescent assay was performed using CellTiter-Glo reagents (Promega Corporation, U.S.A.). The work solution was obtained by reduction of lyophilized CellTiter-Glo Substrate in CellTiter-Glo Buffer and heating on a water bath to room temperature. A 100 μL of this solution was added in each well. Then the plate was rotated for 2 min in one plane to cause cell lysis. Upon incubation at room temperature for 10 min, cell luminance was measured with the help of an LM-01T luminometer with Kilia software (Immunotech, Beckman Coulter Company, Praha, Czech Republic). Measurement results were presented in relative luminescence units (RLU).

Dehydrogenase activity was determined by the MTT-assay using the yellow tetrazolium dye 3-(4,5-dimethylthiazol-2-yl)-2,5-diphenyltetrazolium bromide (Sigma Aldrich, St. Louis, Missouri, U.S.A.), which is

[1] It is worth mentioning that at according to some experimental data the nanoparticle's shape can prove one of factors determining its toxicity 'Raman et al. (2016).

[2] To be sure, it still is but a simplified model because the real extracellular matrix strongly influencing the *in vivo* NP – cell interactions "represents a complex network of variously modified proteins and the glycosaminoglycan, hyaluronan, highly organized in a form of a suprastructure which ultimately constitutes the cell microenvironment" Engin et al. (2017).

[3] This dosage range and the length of cells incubation with NPs were chosen as optimal based on our previous experience and tested in a pilot trial.

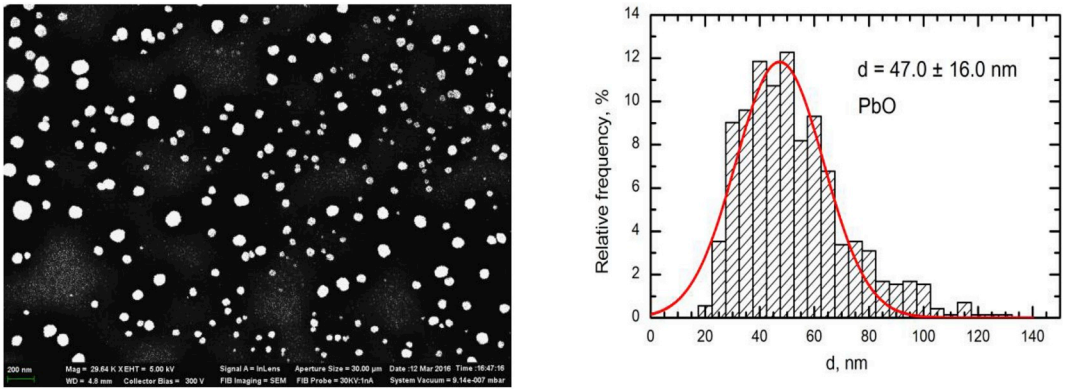

Fig. 1. Scanning electron microscopy (SEM) images of PbO nanoparticles prepared for the experiment (magnification *29640) and particle size distribution function obtained by analysis of SEM images (first published in Minigalieva et al., 2017c).

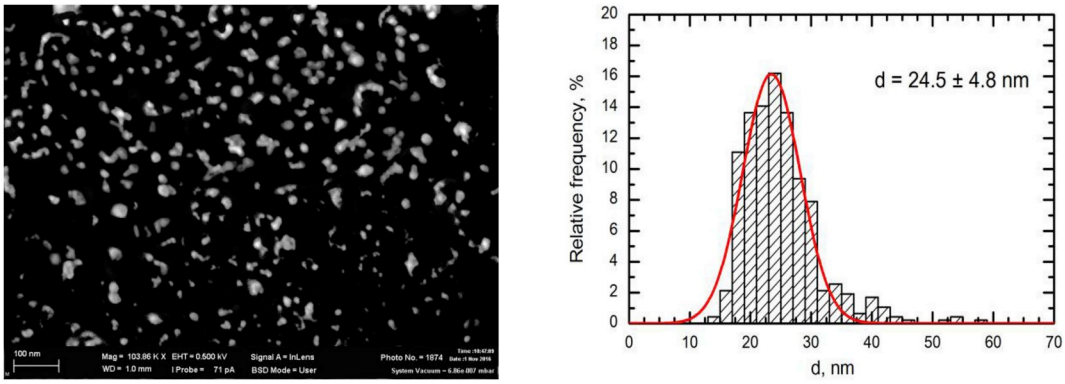

Fig. 2. Scanning electron microscopy (SEM) images of CuO nanoparticles prepared for the experiment (magnification *103,8600) and particle size distribution function obtained by analysis of SEM images (first published in Minigalieva et al., 2017c).

reduced in live cells to purple formazan. The dissolving component was dimethyl sulfoxide (DMSO). We added 20 μL of the dye at a concentration of 5 mg/mL in each well with cells and incubated for 2 h. After this, all of the medium was removed from the plates, and 100 μL of DMSO was added in each well to dissolve the formazan crystals. Optical density was measured by a spectrophotometer, Epoch™ (BioTek, Winooski, Vermont, U.S.A.), at a wavelength of 490 nm. The results were calculated by the formula:

Dehydrogenase activity (%) j 100 x (A490nmsample -A490nmblank)/ (A490nmcontrol - A490nmblank)

Dehydrogenase activity (%) = 100 * (A490nm sample – A490nm blank)/(A490nm control – A490nm blank), where A490nm is the optical density of a sample at a wavelength of 490 nm, blank is the culture medium, for determining the culture medium background, *control* is the culture medium containing no cells, *sample* is cells in the medium with nanoparticles added in various concentrations.

The cell index was estimated on an RTCA iCELLigence™ real-time cell analyzer by ACEA Biosciences, San Diego, California, U.S.A. This instrument uses biosensor electrodes submersed in each individual well. Cells adhere to the surface of the electrode and act as an insulator, increasing electrical impedance Cimpan et al. (2013). Damage to cells reduces their ability to proliferate and to adhere and thus causes the impedance to decrease. The results are expressed as a Normalized Cell Index (NCI) in accordance with the manufacturer's recommendations [Calculation principles of RTCA Software, ACEA Biosciences, U.S.A.]:

Normalized Cell Index (NCI(t)) is calculated as the Cell Index (CI) at a given time point t (CI(t)) divided by the Cell Index at the selected normalization time point (CI($t_{normalization}$) which, in our case, was the instance of nanoparticle addition as follows:

$NCI_{well\_i}(t) = CI_{well\_i}(t)/CI_{well\_i}(t_{normalization})$ with $CI_{well\_i}(t_{normalization}) \neq 0$ and i = 1, 2, … n where NCI_{well_i} (t) is the Normalized Cell Index of well *i* at time point *t*, CI_{well_i} (t) is the Cell Index of well i at time point *t*, $CI_{well\_i}(t_{normalization})$ is the Cell Index of well i at normalization time $t_{normalization}$.

2.3. Mathematical processing and modeling of results

The results were first processed to construct functions approximating the dependence of the cytotoxic effect on the dose of CuO-NP or PbO-NP. Preliminary visual assessment of the plots for the most adequate model suggested choosing a linear $Y = b_0 + b_1X$, log-linear $Y = \exp(b_0 + b_1X)$ or hyperbolic $Y = \frac{b_0 + b_1X}{b_2 + b_3X}$ function. The coefficients b_i of these functions were obtained with the help of the least squares method using the experimental data. Since the coefficients thus found proved to be statistically highly significant for all the mathematical models compared, we used the same criterion of minimality of the sum of squared deviations of the observed values from the model predictions, which justified choosing in all cases the hyperbolic function as the best adequate model of dose-response relationships.

As well as in our previous works on combined toxicity (Varaksin et al., 2014; Katsnelson et al., 2015a; 2015b; Minigalieva et al., 2017a,b,c), we performed mathematical modeling of the combined CuO–PbO action by the Response Surface Methodology (RSM).

The regression equation describing the response surface Y = Y (x_1, x_2) in our case is:

$$Y = b_0 + b_1x_1 + b_2x_2 + b_{12}x_1x_2 \quad (1)$$

where Y is a cytotoxicity index, and x_1 and x_2 are the doses of the agents

participating in the combination (CuO and PbO, respectively). This equation may be constructed by fitting the coefficients b_0, b_1, b_2 and b_{12} to experimental data. It is inferred that two agents produce a unidirectional effect on response Y if both one-way response functions Y (x_1, 0) and Y (0, x_2) either increase or decrease with an increase in x_1 or x_2; on the contrary, two agents are assumed to be acting contra-directionally if one function increases while the other decreases. It should be stressed that, according to the response surface approach, even in the case of two-level agents, model (1) enables one to predict the magnitude of response Y for any combination of agent doses within the experimental range for each of them (rather than at two points only).

Actual experimental values were employed to obtain Equation (1) for a corresponding index Y using the ordinary least squares method.

3. Results and discussion

Theoretically, a quantitative relationship between the magnitude (specifically, toxicant dose or concentration) of an assumingly damaging impact on a living system and the value of some index of this system's status is an important argument in favor of the assumption that a shift in this index could be attributed to this impact. At the same time, analysis of dose-effect or dose-response relationships is of practical importance both in terms of health risk assessment and management and from the perspective of experimental toxicology for selecting a range of doses within which to conduct further investigations. For instance, it seems most reasonable to model the combined cytotoxicity of two MeO-NP species on a cell culture using the concentrations of each of them acting alone which are explicitly effective according to the toxic effect's index used, whereby even a relatively small increase in the concentration increases the shift in this index considerably.

The first step in our study was, therefore, experimental and mathematical modeling of one factor dose-response dependencies for each of the three cytotoxicity indices used. The results of this step are shown graphically in Figs. 3–5, comparing actual data with their approximant hyperbolic function. As was pointed out above in Section 2.3, this approximation proved to be closer than the linear or log-linear ones. Note that although practical conclusions from the analysis concerning the choice of effective doses did not depend on which function was used, the hyperbolic one confirms the general observation that the dose-effect dependence is quasi-linear within only a limited range of doses. In this respect, the outcomes of this study are, in principle, consistent with the results of the previous one that involved NiO-NP and Mn3O4-NP (Minigalieva et al., 2017a).

We can see that in each of the three cytotoxicity tests the dose-response dependence under consideration displayed the same common pattern for both CuO-NP and PbO-NP. This conclusion is now even more unequivocal than when it was based on the previous experiments (Minigalieva et al., 2017a). Moreover, the fact that the effective dose range was found to be the same for the various indices of the effect is interesting theoretically as it confirms that all the three indices reflect the degree of cytotoxic damage to the cell although they have different underlying biochemical and biophysical mechanisms. At the same time, the combined cytotoxicity type revealed in this range proved to be dependent on which index it was assessed by.

Indeed, as follows from the isobolograms obtained with the help of the Response Surface Method (Fig. 6), the estimates of the cytotoxicity effect by the MTT-assay and NCI reveal a unidirectional action tending towards subadditivity in the first case and displaying explicit subadditivity in the second. However, the luminescence index suggests that the conclusion concerning the type of combined action displayed by the MeO-NPs under study is far from being unequivocal. In this case, the subadditive type of unidirectional combined toxicity manifested itself only at the lowest doses of both agents while higher doses, of at least one of them, resulted in different variants of contra-directional action.

It should be emphasized that in a whole range of *in vivo* experiments (see the overview publications Katsnelson et al. (2017); Minigalieva et al., 2017b, and in our previous study on cell cultures Minigalieva et al. (2017a), we developed an evidence base for assuming, as one of the paradigms of the combined toxicity theory, just the typological multiplicity of combined toxicity displayed by one and the same pair of toxicants depending, first of all, on the effect estimated, as well as on its level and dose ratio. The examples of such multiplicity relating exactly to an animal experiment with the [CuO-NP + PbO-NP] combination are represented by the isobolograms constructed in the data analysis but not shown in the paper reporting its results Minigalieva et al., 2017c.

Out of the multitude of isobolograms, we show in Fig. 7 only the ones whose isobole shapes and slopes are similar to the combined cytotoxicity typology identified on a cell culture (cf. Fig. 6). Thus, in particular, it demonstrates: the additivity of the unidirectional action on the platelet count; some tendency towards the subadditivity of the unidirectional action on the general motor activity of rats (judging by the number of squares crossed in 3 min); and the typical dependence of the combined toxicity type estimated by an increase in the concentration of uric acid in the blood on effect level and dose ratio. In the latter case, it varies from antagonism (as subadditivity of unidirectional action or even as contra-directional action) to synergism (superadditivity).

On the whole, in the subchronic animal experiment under consideration the isobolograms of the type shown in Fig. 7a were obtained

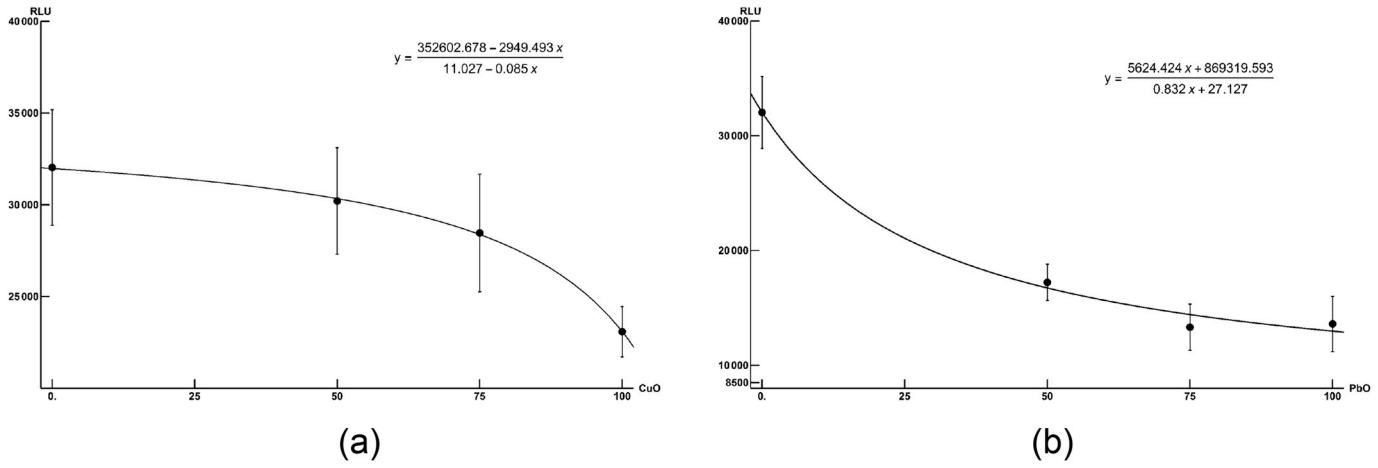

Fig. 3. The dose-response dependence of the reduction of the intensity of the luminescent signal from the cell culture (axis Y, in Relative Light Units) on the concentration of (a) CuO-NP or (b) PbO-NP in the medium (axis X, in μg/mL).

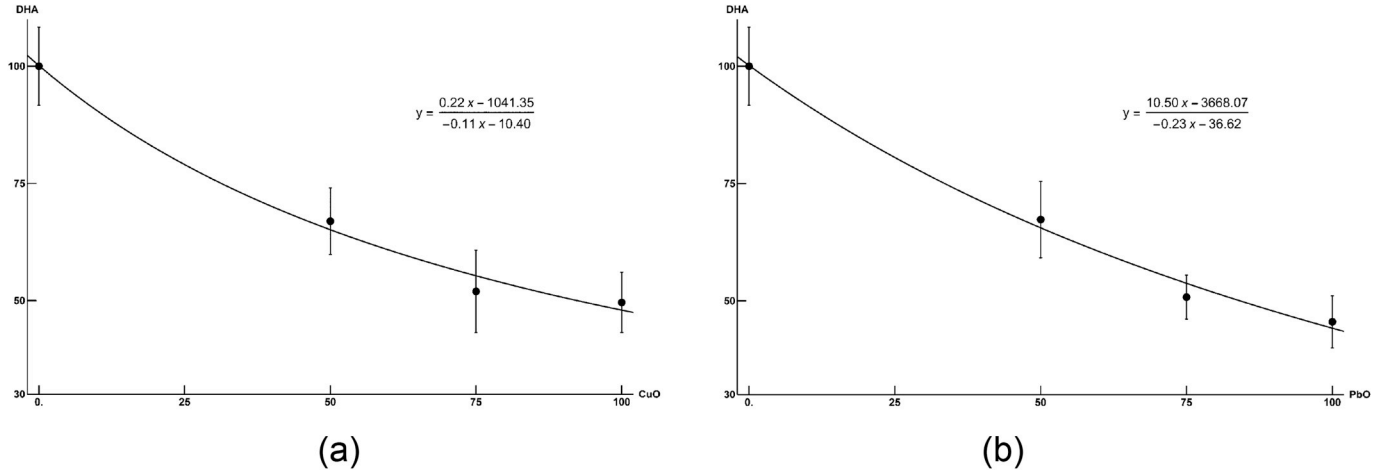

Fig. 4. The dose-response dependency of the reduction of the dehydrogenase activity (DHA) in the cell culture medium (Y, absorbance units expressed as %% of controls) on the concentration of (a) CuO-NP or (b) PbO-NP in the medium (axis X, in μg/mL).

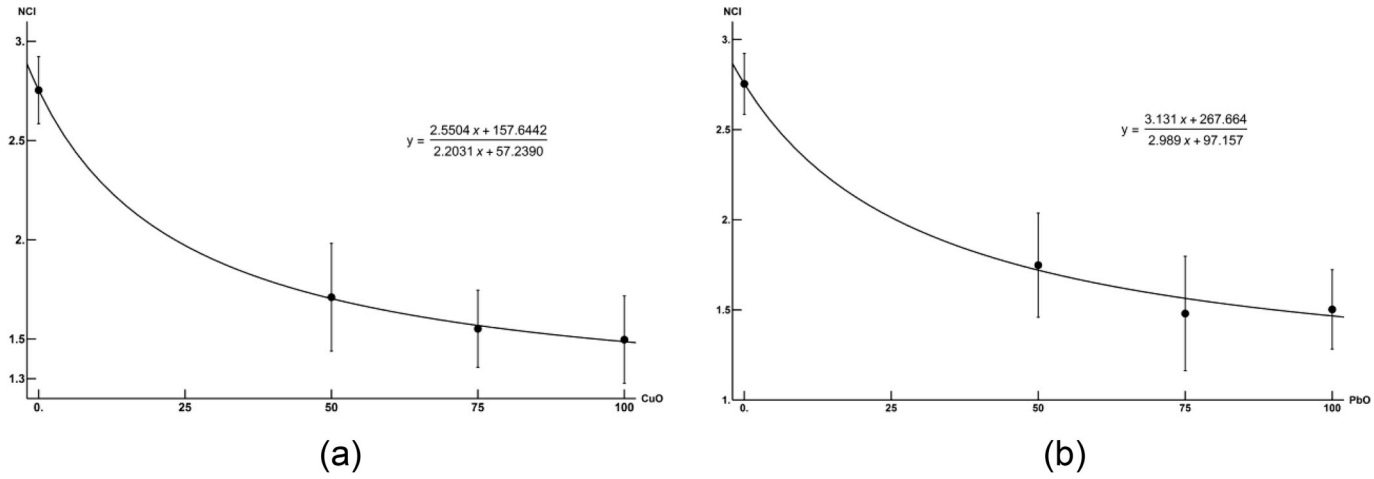

Fig. 5. The dose-response dependence of the reduction of the Normalized Cell Index in the cell culture (axis Y, in dimensionless numbers) on the concentration of (a) CuO-NP or (b) PbO-NP in the medium (axis X, in μg/mL).

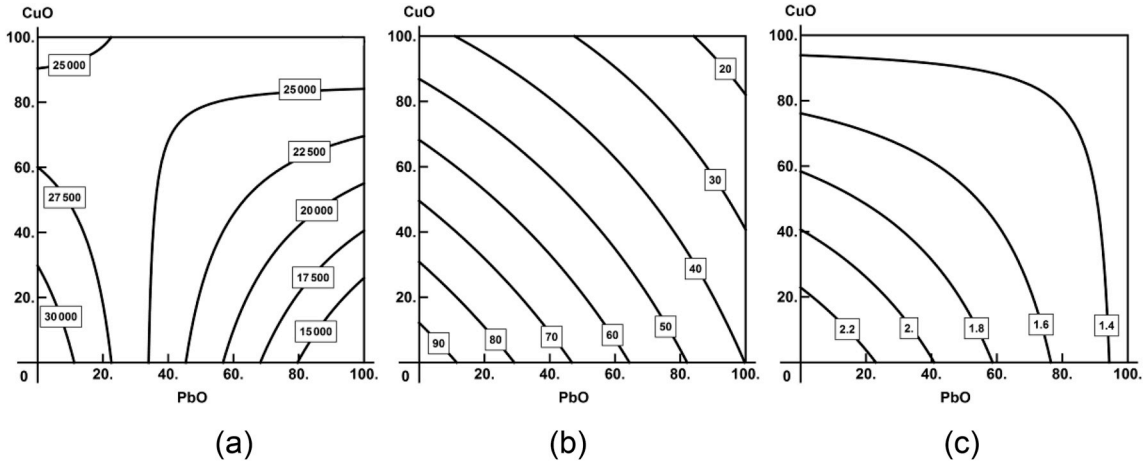

Fig. 6. Isobolograms characterizing the combined toxic action of CuO-NP and PbO-NPs in experiments on the fibroblast culture as estimated by increase in: (a) the intensity of the luminescent signal, (b) the formazan formation, and (c) Normalized Cell Index. Numbers on axes are respective MeO-NP concentrations in μg/mL, numbers on isoboles are the effect value to which they correspond.

by two effects of combined toxicity, in Fig. 7b by another two effects, and in Fig. 7c by another six effects. We also included one of the isobolograms constructed using the cytological indices of the bronchoalveolar lavage fluid obtained after single-shot intratracheal instillations of the same MeO-NPs separately or in different combinations (Fig. 7d). More specifically, the index in point is 'neutrophil leukocytes to alveolar count' ratio (NL/AM), which, as was shown long ago (starting with Privalova et al., 1980), correlates well with the

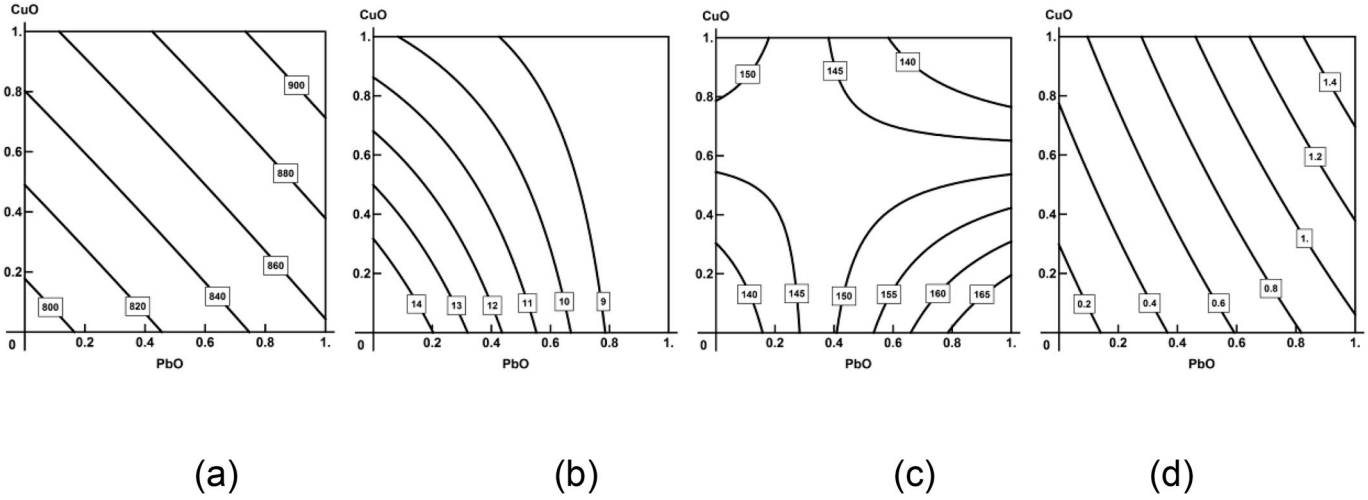

Fig. 7. Isobolograms characterizing the combined toxic action of CuO-NP and PbO-NPs in experiments on rats as estimated after repeated intraperitoneal injections by (a) increase in the blood thrombocyte count; (b) decrease in the number of squares spontaneously crossed during 3 min; (c) increase in the blood uric acid concentration, and after single-shot itratracheal instillation by (d) the neutrophil leukocytes to alveolar count ratio in the bronchoalveolar lavage fluid. Numbers on axes are respective MeO-NP dosage as proportion of the maximal dose used in this experiment, numbers on isoboles are the effect value to which they correspond (NB! Thrombocyte count x10^3). The design of the experiments was described in Minigalieva et al. (2017c).

cytotoxicity of various particles for macrophages *in vitro*. It is therefore interesting that the combined action of CuO-NP and PbO-NP *in vivo* proved to be explicitly additive for this index.

Thus, the variability of the typology of combined cytotoxic action displayed by CuO-NP and PbO-NP *in vitro* is, in general, similar to its variability *in vivo* on system and organism levels. We demonstrated the same when constructing analogous experimental models of combined toxicity for NiO-NP and Mn_3O_4-NP Minigalieva et al. (2017a). We take the liberty of suggesting this as a new confirmation that the multiplicity of combined toxicity types can indeed be considered as a paradigm of the general toxicological theory.

With regard to the case considered in this paper, we can also hypothesize that the similarity of the combined toxicity types determined by the MTT-assay and NCI (Fig. 6b–c) and the difference of the types identified by the intensity of the luminescence signal (Fig. 6a) are not accidental. Rather, they are associated with the similarity or dissimilarity of the mechanisms underlying the development of the effects. Indeed, reduced dehydrogenase activity revealed in the MTT-assay reflects cell death, but the same death leads to the detachment of cells from the electrode surface and thus to a decrease in NCI. By contrast, the intensity of cell luminescence reflects the ATP content of viable cells, which depends on oxidative phosphorylation processes. The latter may also be suppressed to a varying extent and, possibly, enhanced in a part of cells in the culture due to the activating effect of other cells breakdown products.

4. Conclusions

1. Separate damaging effects of PbO and CuO nanoparticles as estimated on an established line of human fibroblast-like cells using three different cytotoxicity indices are similarly dose-dependent. In a practically possible range of nanoparticle concentrations, this dependence can be adequately approximated with the hyperbolic function.

2. At equal exposure levels, the cytotoxicity of PbO-NP compared with that of CuO-NP was found to be quantitatively rather similar, as previously observed by Minigalieva et al. (2017c) for some non-specific *in vivo* toxicity measures of the same nanoparticles.

3. The combined *in vitro* cytotoxicity of PbO-NP and CuO-NP described mathematically using the Response Surface Methodology displayed a variable pattern depending on the index used and, for one of the indices, on the nanoparticle dose ratio as well. This finding corroborates, in this respect also, the previously obtained conclusions from an animal experiment involving the same metal oxide nanoparticles and from *in vitro* and *in vivo* experiments with another pair of nanoparticles (NiO and Mn_3O_4).

Appendix A. Supplementary data

Supplementary data to this article can be found online at https://doi.org/10.1016/j.fct.2019.110753.

References

Alarifi, S., Ali, D., Verma, A., Alakhtani, S., Ali, B.A., 2013. Cytotoxicity and genotoxicity of copper oxide nanoparticles in human skin keratinocytes cells. Int. J. Toxicol. 32, 296–307.

Amiri, A., Mohammadi, M., Shabani, M., 2016. Synthesis and toxicity evaluation of lead oxide (PbO) nanoparticles in rats. Electron. J. Biol. 12, 2.

Ávalos, A., Haza, A.I., Mateo, D., Morales, P., 2018. In vitro and in vivo genotoxicity assessment of gold nanoparticles of different sizes by comet and SMART assays. Food Chem. Toxicol. 120, 81–88.

Bondarenko, O., Ivask, A., Käkinen, A., Kahru, A., 2012. Sub-toxic effects of CuO nanoparticles on bacteria: kinetics, role of Cu ions and possible mechanisms of action. Environ. Pollut. 169, 81–89.

Cimpan, M.R., Mordal, T., Schölermann, J., Allouni, Z.E., Pliquett, U., Cimpan, E., 2013. An impedance-based high-throughput method for evaluating the cytotoxicity of nanoparticles. J. Phys. Conf. Ser. 429 012026, 1-10.

Cronholm, P., Karlsson, H.L., Hedberg, J., Lowe, T.A., Winnberg, L., Elihn, K., Wallinder, I.O., Möller, L., 2013. Intracellular uptake and toxicity of Ag and CuO nanoparticles: a comparison between nanoparticles and their corresponding metal ions. Small 8, 970–982.

Cuillel, M., Chevallet, M., Charbonnier, P., Fauquant, C., Pignot-Paintrand, I., Arnaud, J., Cassio, D., Michaud-Soret, I., Mintz, E., 2014. Interference of CuO nanoparticles with metal homeostasis in hepatocytes under sub-toxic conditions. Nanoscale 16, 1707–1715.

Dumková, J., Smutná, T., Vrlíková, L., Le Coustumer, P., Večeřa, Z., Dočekal, B., Mikuška, P., Čapka, L., Fictum, P., Hampl, A., Buchtová, M., 2017. Sub-chronic inhalation of lead oxide nanoparticles revealed their broad distribution and tissue-specific subcellular localization in target organs. Part. Fibre Toxicol. 14 (1), 55.

Engin, A.B., Nikitovic, D., Neagu, M., Henrich-Noack, P., Docea, A.O., Shtilman, M.I., Golokhvast, K., Tsatsakis, A.M., 2017. Mechanistic understanding of nanoparticles' interactions with extracellular matrix: the cell and immune system. Part. Fibre Toxicol. 14, 22.

Fernández-Bertólez, N., Costa, C., Brandão, F., Kiliç, G., Duarte, J.A., Teixeira, J.P., Pásaroa, E., Valdiglesias, V., Laffon, B., 2018. Toxicological assessment of silica-coated iron oxide nanoparticles in human astrocytes. Food Chem. Toxicol. 118, 13–23.

Ghosh, M., Sinha, S., Jothiramajayam, M., Jana, A., Nag, A., Mukherjee, A., 2016. Cytogenotoxicity and oxidative stress induced by zinc oxide nanoparticle in human lymphocyte cells in vitro and Swiss albino male mice in vivo. Food Chem. Toxicol. 97,

286–296.
Gomes, T., Araújo, O., Pereira, R., Almeida, A.C., Cravo, A., Bebianno, M.J., 2013. Genotoxicity of copper oxide and silver nanoparticles in the mussel Mytilus galloprovincialis. Mar. Environ. Res. 84, 51–59.
Henrich-Noack, P., Nikitovic, D., Neagu, M., Docea, A.O., Engin, A.B., Gelperina, S., Shtilman, M., Mitsias, P., Tzanakakis, G., Gozes, I., Tsatsakis, A., 2019. The blood–brain barrier and beyond: nano-based neuropharmacology and the role of extracellular matrix. Nanomed. Nanotechnol. Biol. Med. 17, 359–379.
Karlsson, H.L., Cronholm, P., Gustafsson, J., Möller, L., 2008. Copper oxide nanoparticles are highly toxic: a comparison between metal oxide nanoparticles and carbon nanotubes. Chem. Res. Toxicol. 21, 1726–1732.
Katsnelson, B.A., Privalova, L.I., Sutunkova, M.P., Minigalieva, I.A., Gurvich, V.B., Shur, V.Y., Shishkina, E.V., Makeyev, O.H., Valamina, I.E., Varaksin, A.N., et al., 2017. Experimental research into metallic and metal oxide nanoparticle toxicity in vivo. In: Yan, B., Zhou, H., Gardea-Torresdey, J. (Eds.), Bioactivity of Engineered Nanoparticles. Springer, New York, NY, USA, pp. 259–319 (Chapter 11).
Kirichenko, K. Yu., Agoshkov, A.I., Drozd, V.A., Gridasov, A.V., Kholodov, A.S., Kobylyakov, S.P., Kosyanov, D. Yu., Zakharenko, A.M., Karabtsov, A.A., Shimanskii, S.R., Stratidakis, A.K., Mezhuev, Ya.O., Tsatsakis, A.M., Golokhvast, K.S., 2018. Characterization of fume particles generated during arc welding withvarious covered electrodes. Sci. Rep. 8 (1), 1–9. https://doi.org/10.1038/s41598-018-35494-1.
Magaye, R., Zhao, J., Bowman, L., Ding, M., 2012. Genotoxicity and carcinogenicity of cobalt-, nickel- and copper-based nanoparticles. Exp. Ther. Med. 4, 551–561.
Minigalieva, I.A., Bushueva, T.V., Froehlich, E., 2017a. Are in vivo and in vitro assessments of comparative and combined toxicity of the same metallic nanoparticles compatible, or contradictory, or both? A juxtaposition of data obtained in respective experiments with NiO and Mn_3O_4 nanoparticles. Food Chem. Toxicol. 109, 393–404. https://doi.org/10.1016/j.fct.2017.09.032.
Minigalieva, I.A., Katsnelson, B.A., Panov, V.G., Varaksin, A.N., Gurvich, V.B., Privalova, L.I., Sutunkova, M.P., Klinova, S.V., 2017b. Experimental study and mathematical modeling of toxic metals combined action as a scientific foundation for occupational and environmental health risk assessment. A summary of results obtained by the Ekaterinburg research team (Russia). Toxicol. Rep. 4C, 194–201.
Minigalieva, I.A., Katsnelson, B.A., Panov, V.G., Privalova, L.I., Varaksin, A.N., Gurvich, V.B., Sutunkova, M.P., Shur, V.Ya., Shishkina, E.V., Valamina, I.E., Zubarev, I.V., Makeyev, O.H., Meshtcheryakova, E.Y., Klinova, S.V., 2017c. In vivo toxicity of copper oxide, lead oxide and zinc oxide nanoparticles acting in different combinations and its attenuation with a complex of innocuous bio-protectors. Toxicology 380, 72–93.
Miri, A., Sarani, M., Hashemzadeh, A., Mardani, Z., Darroudi, M., 2018. Biosynthesis and cytotoxic activity of lead oxide nanoparticles. Green Chem. Lett. Rep. 11 (4), 567–572.
Neagu, M., Piperigkou, Z., Karamanou, K., Engin, A.B., Docea, A.O., Constantin, C., Negrei, C., Nikitovic, D., Tsatsakis, A., 2017. Protein bio-corona: critical issue in immune nanotoxicology. Arch. Toxicol. 91 (3), 1031–1048. https://doi.org/10.1007/s00204-016-1797-5.
Ng, D., Chu, Y., Tan, S., Wang, S., Lin, Y., Chu, C., Soo, Y., Song, Y., Chen, P., 2019. In vivo *evidenc*e of intestinal lead dissolution from lead dioxide (PbO2) $nano_p$articles and resulting bioaccumulation and toxicity in medaka fish. Environ. Sci.: Nano 6, 580–591.
Pang, C., Selck, H., Misra, S.K., Berhanu, D., Dybowska, A., Valsami-Jones, E., Forbes, V.E., 2012. Effects of sediment-associated copper to the deposit-feeding snail, Potamopyrgus antipodarum: a comparison of Cu added in aqueous form or as nano- and micro-CuO particles. Aquat. Toxicol. 15, 114–122.
Piperigkou, Z., Karamanou, K., A.B., Gialeli, Ch, Vynios, D.,M., Pavão, M.S.G., Golokhvast, K.S., Shtilman, M.I., Argiris, A., Shishatskaya, E., Tsatsakis, A.M., 2016. Emerging aspects of nanotoxicology in health and disease: from agriculture and food sector to cancer therapeutics. Food Chem. Toxicol. 91, 42–57.
Privalova, L.I., Katsnelson, B.A., Loginova, N.V., Gurvich, V.B., Shur, V.Y., Valamina, I.E., Makeyev, O.H., Sutunkova, M.P., Kozin, R.V., Meshtcheryakova, E.Y., Korotkov, A.V., Shuman, E.A., Zvereva, A.E., Kostykova, S.V., 2014. Subchronic toxicity of copper oxide nanoparticles and its attenuation with the help of a combination of bioprotectors. Int. J. Mol. Sci. 15, 12379–12406.
Privalova, L.I., Katsnelson, B.A., Osipenko, A.B., Yushkov, B.H., Babushkina, L.G., 1980. Response of a phagocyte cell system to products of macrophage breakdown as a probable mechanism of alveolar phagocytosis adaptation to deposition of particles of different cytotoxicity. Environ. Health Perspect. 35, 205–218.
Raman, V., Suresh, Sh., Savarimuthu, Ph.A., Raman, Th, Tsatsakis, A.M., Golokhvast, K.S., Vadivel, V.K., 2016. Synthesis of Co_3O_4 nanoparticles with block and sphere morphology, and investigation into the influence of morphology on biological toxicity. Exp. Ther. Med. 11, 553–560.
Sizova, E., Miroshnikov, S., Polyakova, V., Gluschenko, N., Skalny, A., 2012. Copper nanoparticles as modulators of apoptosis and structural changes in tissues. J. Biomaterials Nanobiotechnol. 3 97–10.
Studer, A.M., Limbach, L.K., van Duc, L., Krumeich, F., Athanassiou, E.K., Gerber, L.C., Moch, H., Stark, W.J., 2010. Nanoparticle cytotoxicity depends on intracellular solubility: comparison of stabilized copper metal and degradable copper oxide nanoparticles. Toxicol. Lett. 1, 169–174.
Tsatsakis, A., Kouretas, D., Tzatzarakis, M., Stivaktakis, P., Tsarouhas, K., Golokhvast, K., Rakitskii, V.N., Tutelyan, V.A., Hernandez, A.F., Rezaee, R., Chung, G., Fenga, C., Engin, A.B., Neagu, M., Arsene, A.L., Docea, A.O., Gofita, E., Calina, D., Taitzoglou, I., Liesivuori, J., Hayes, A.W., Gutnikov, S., Tsitsimpikou, C., 2016. Simulating real-life exposures to uncover possible risks to human health: a proposed consensus for a novel methodological approach. Hum. Exp. Toxicol. 36, 554–564.
Tsatsakis, A., Goumenou, M., Liesivuori, J., Dekant, W., Hernández, A.F., 2018. Toxicology for real-life risk simulation - editorial preface to this special issue. Toxicol. Lett. 309, 33–34.
Xu, J., Li, Z., Xu, P., Xiao, L., Yang, Z., 2013. Nanosized copper oxide induces apoptosis through oxidative stress in podocytes. Arch. Toxicol. 87, 1067–1073.